Proceedings World Geothermal Congress 2015
Melbourne, Australia, 19-25 April 2015

Microearthquake (MEQ) Investigation Reveals the Sumatran Fault System in Hululais Geothermal Field, Bengkulu, Indonesia

Aditya A. Juanda, Astha D. K. Wardhani, and Imam B. Raharjo

PT Pertamina Geothermal Energy, Skyline Building 15th Floor, Jl. M. H. Thamrin No. 9, Jakarta

adityajuanda@pertamina.com

Keywords: Sumatran fault system Musi and Ketaun segment, Hululais geothermal field, microearthquake (MEQ), single event determination, joint hypocenter determination

ABSTRACT

Hululais field is located in Bengkulu province, about 30 km north of the Bengkulu city. During April to July 2012, microearthquake (MEQ) monitoring was undertaken for about 120 days consisting of 6 surface stations (three channels each, 4.5 Hz natural frequency and 200 sps sampling rate). Many events were detected with magnitude ranging from M 0.1 up to M 2. The P and S wave arrival times of each event are manually revised. The locations of the hypocenters are determined by applying the Single Event Determination (SED) and Joint Hypocenter Determination (JHD) techniques.
The hypocenter distributions from both techniques are similar however the JHD results have smaller RMS error. The hypocenter distribution pattern depicts the Sumatran fault system with its associated faults within Musi and Ketaun segment that dominantly have a NW – SE trend. Three clusters of hypocenter are observed with depth varying from 1 to 10 km. One of the MEQ clusters depicts a faulted or fractured zone from the Musi segment. There are also two clusters that clearly show fault systems in Ketaun segment. One has a similar orientation as fault plane in the Musi segment, and the other has opposite orientation with a similar dip magnitude. The clusters of faults are regarded as high permeable regions. These fault regions have been the main target for exploration drilling in Hululais field.

1. INTRODUCTION

Indonesia is considered to have one of the world's largest geothermal potential. PT Pertamina Geothermal Energy (PGE) has been appointed by the Indonesia government, to operate 14 geothermal fields in Indonesia. For Sumatra Island alone, PGE has contracts to operate Sibayak (north Sumatra), Kerinci (Jambi), Lumut Balai (south Sumatra), Hululais (Bengkulu) and Ulubelu (Lampung). All of those geothermal potentials are situated along the Sumatran fault. The Hululais field is PT PGE's highest priority of all the target areas to be explored and exploited. Exploration activities such as gravity, magnetotelluric (MT) measurements and surface geological mapping altogether with geochemistry surveys have been done in Hululais field. Based on previous study (Sieh K. and Natawidjaja, D., 2000) the Sumatran fault is defined as dextral slip fault type and highly correlated with the active volcanic arc along the fault itself. The Sumatran fault is divided into 19 segments and Hululais field is situated within two segments, the Musi and Ketaun segments. Since Hululais is situated in a region with intensive seismic activity,,during April to July 2012 the microearthquake (MEQ) monitoring was undertaken to monitor local seismic sources covering the Hululais field and also the Sumatran fault on the eastern side. In this paper we compare the hypocenter determination results from Single Event Determination (SED) and Joint Hypocenter Determination (JHD) techniques which the P and S wave arrival times of each event are manually picked. We investigate three clusters of hypocenter that depict the Sumatran fault patterns with its associated faults within Musi and Ketaun segment.

Although most of the MEQ monitoring application is to investigate fracture swarms from production and injection activity (active sources), there is also possibility of using MEQ data to investigate faults or fractures regions from passive sources (tectonic, faults, fractures) in exploration field. This study is required to identify seismogenic (seismically active) regions which describe good permeability faults or fractures within the area. Therefore, a comprehensive characterization of the faults or fractures regions is required because the regions have been regarded as the main target due to a successful exploration drilling in Hululais field.

2. LOCATION

Hululais field is located in Bengkulu province, about 30 km north of the Bengkulu city (Figure 1).

3. GEOLOGICAL SETTINGS

Hululais is situated on the west part of the Sumatran fault. Sieh K. and Natawidjaja, D. (2000) describe the 1900 km long Sumatran fault as a dextral slip that accommodates a significant amount of oblique convergence between the Eurasian and Indo-Australian plates. Based on geodetic measurement, it was suggested that slip along the Sumatran fault is almost uniform at about 25 mm/year. However, this rate movement is not consistent with the direct measurement from geological slip rate which is at 27 and 11 mm/year. The changing of rate and direction of the Indo-Australian plate motion phenomena causes right step-over segmentation along the Sumatran fault. Figure 1 describes the Sumatran fault system in regional scale with dominant direction trending NW – SE (Muraoka et al., 2010).

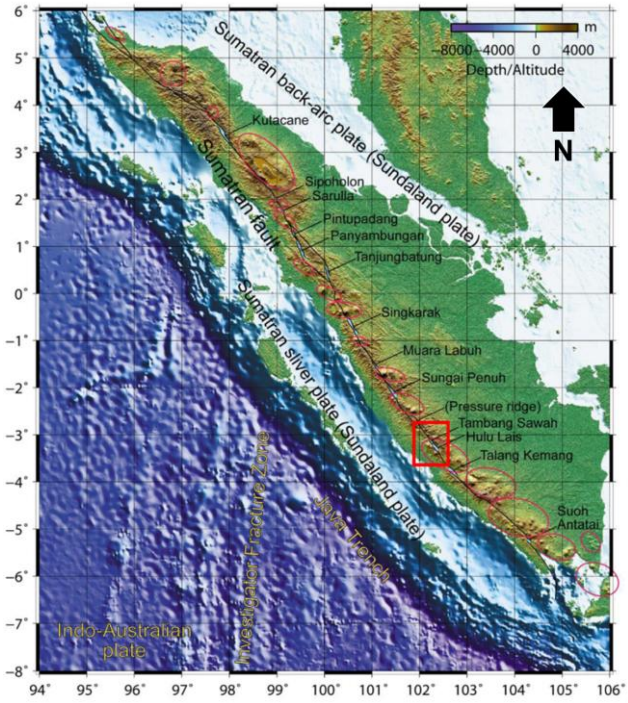

Figure 1 Regional scale of the Sumatran fault system. The Hululais field location is indicated by the red rectangle shape (modified from Muraoka et al., 2010).

The Sumatran fault is divided into 19 segments and Hululais field is situated within two segments, they are Musi and Ketaun segment (Figure 2). The Musi segment is described as a 70 km long segment that consists of several highly discontinuous fault segments and the slip rate for this segment is 11 mm/year (Sieh K. and Natawidjaja, D., 2000). The Ketaun segment is described as an 85 km long segment that consists of fault trace with discontinuities and dilatational step-overs for about a kilometer in dimension. The southern end part of the Ketaun segment is step-over onto the Musi segment for about 6 – 8 km wide whereas the northern end part of the Ketaun segment is a contractional step-over (pressure ridge) (Sieh K. and Natawidjaja, D., 2000). The step-over phenomena leads to the presence of the Hululais pull-apart basin between Musi and Ketaun segment. These phenomena play an important role for geothermal system development in Hululais field. Along the Sumatran fault, the hot fluid discharge is associated with the pull-apart basin and also with the volcanic activities (Muraoka et al., 2010). Therefore the geothermal fields in Sumatra are mostly developed along the fractures along the Sumatran fault.

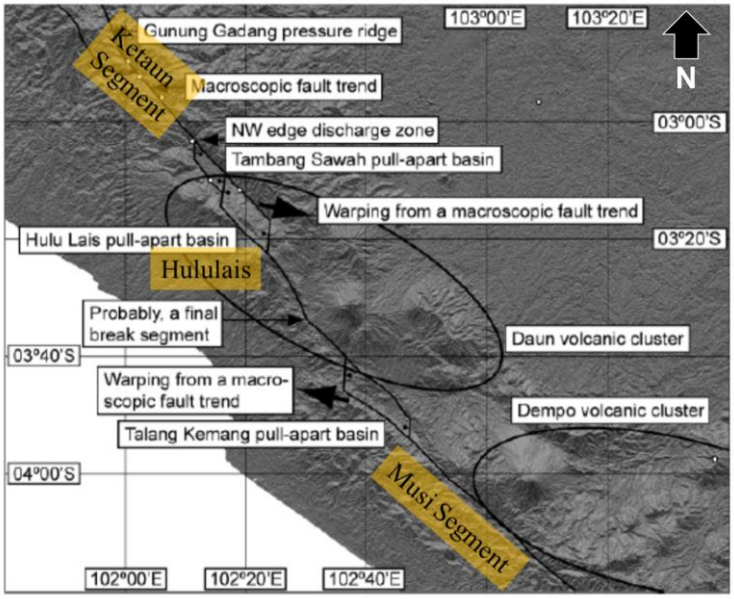

Figure 2 Musi and Ketaun segment Hululais field. Right step over phenomena of Musi and Ketaun segment (modified from Muraoka, et al., 2010).

4. MICROEARTHQUAKE (MEQ) FIELD CAMPAIGN

4.1 MEQ Network Configurations

During April to July 2012 (120 days) we installed 6 surface geophones with three components sensors, 4.5 Hz natural frequency and recorded the signals by using the 24-bit SMART-24® series digitizer recorder with sampling at 200 samples per second (sps). The 6 sensors were buried at about 2 meters depth. The spacing between sensors is around 6 km and the network covered the entire Hululais field and also the Sumatran fault regions on the eastern side of the field (Figure 3). With this network range, it is expected that we could detect the natural seismic or microearthquake activity of the Sumatran fault in the vicinity of the Hululais geothermal field.

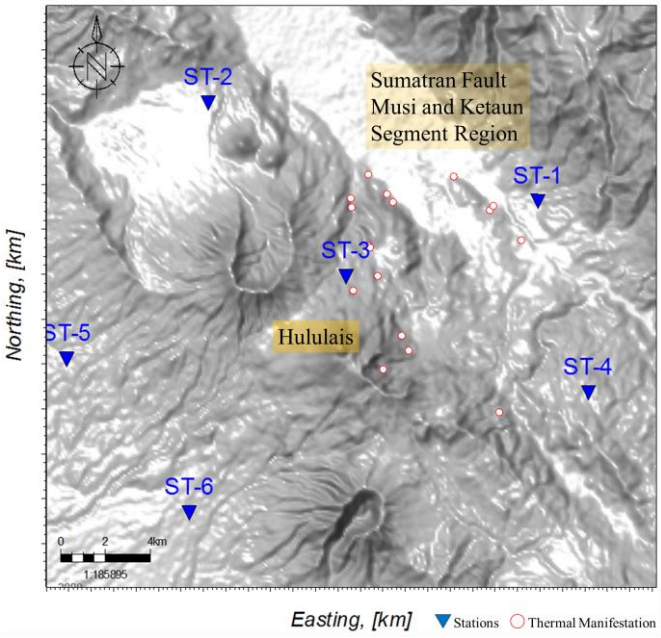

Figure 3 MEQ Network in Hululais geothermal gield. The MEQ stations are indicated by blue triangles whereas the thermal manifestations are indicated by red circles.

4.2 Noise Level Analysis

Most of the MEQ station sites (ST) are situated in relatively remote areas and only accessible by motorcycle. Based on our experience in operating the SMART-24 ® Instruments, we define noise level category at site as high and low. The amplitude threshold was defined as 13 count peak. If sites having amplitude lower than 13 count peak, then it will be defined as low noise site category and vice versa. These categories define the sites' quality for geophone deployment purpose, where the high and low noise level indicates poor and excellent site quality, respectively. The graph in Figure 4 illustrates the amplitude signal (average) in function of time. We sampled 24-hours recording data from all the 6 stations. Based on the graph, it clearly seen that generally the noise level at day is relatively higher than at night except at ST-5 and ST-6 where the amplitude between day and night are similar.

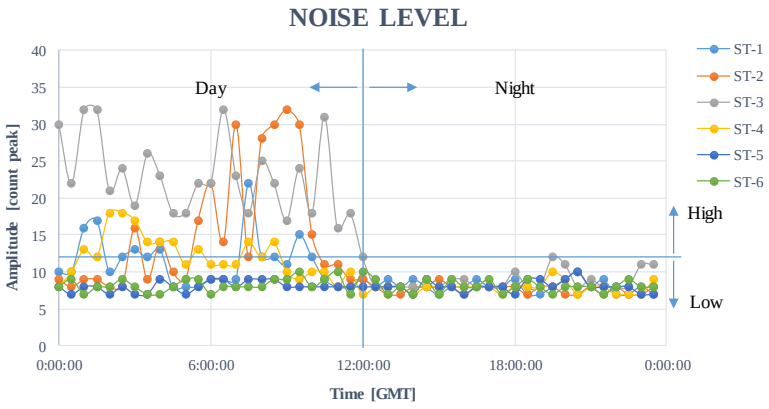

Figure 4 Noise level at site, showing noise level during day and night time. Based on the graph, noise level during the day is relatively higher than at night except at ST-5 and ST-6.

In more details, the amplitude noise level average at ST-1 at day and night time is 10 count peak. At site ST-2, the amplitude average is about 12 count peak. Site ST-3 has a very distinct characteristic where the amplitude average is 17 count peaks. Similar to ST-1, the amplitude average at site ST-4 is 10 count peaks. The lowest amplitude noise level, at site ST-5 and ST-6, the averaged about 8 count peak during the day and about 8 count peak during the night. Based on these data, we can define that all of the sites are categorized as an excellent quality site for geophone deployment with note that the ST-3 has a relatively higher noise level. This

implies that the signal to noise (S/N) ratio at ST-3 is lower than the other sites. Table 1 describes the complete calculation of average amplitude (count peak) at each site.

Table 1 Average amplitude (count peak) at each site

Station ID	Average Amplitude (count peak)		
	Day	Night	Combine
ST-1	12	8	10
ST-2	16	8	12
ST-3	24	10	17
ST-4	12	8	10
ST-5	8	8	8
ST-6	8	8	8

5. DATA AND PROCESSING PROCEDURE

5.1 Data Selection

During 120 days of recording, more than 180 earthquake events were detected. The P and S wave arrival times were detected using the automatic picking routine based on the SAPS seismological data acquisition and processing system that utilized in the SMARTQuake® program (Oncescu, M.C., et al., 1996). This routine simply picks all clear onset on the P and S wave arrival times from local and regional events. The SMARTQuake® software is using a robust location program, called HYPOPLUS (Oncescu, M.C. and Rizescu, M., 1997) working in automatic mode. Then we apply restriction criteria to obtain the local earthquakes only. The selection criteria are simply select earthquakes that have difference of arrival time between S and P wave less than 3 seconds. For the picking purpose, there is an additional restriction that we only used events recorded by at least 4 stations. This restriction criteria reduced the number of data down to about 53 events containing about 960 observed P and S wave arrivals time phases picking.

5.2 Velocity Structure

The 1-D layered velocity structure variation is simply defined based on the distribution of lithology from well drilling information. However the P and S wave velocity values are generalized for certain lithology. The information from well cuttings describe sequences of the lithology from surface to total depth of well penetration (TD). Generally, the lithology variation is volcanic products such as Breccia, Andesite and Tuff. However for the section deeper than TD we set an increasing velocity trend downwards to Moho discontinuity. For this study, we use ratio of Vp / Vs = 1.73. The velocity structure that we use in this study is illustrated is Figure 5.

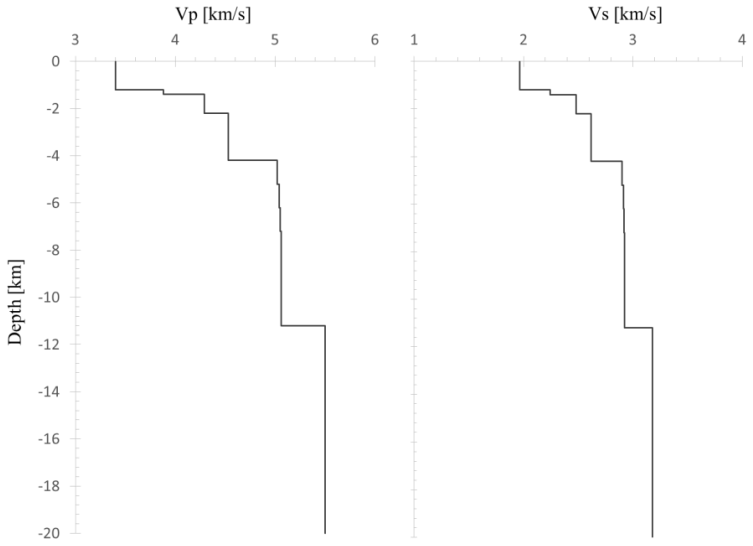

Figure 5 P and S velocity structure used in this study with Vp/Vs ratio = 1.73.

5.3 Manual Phase Picking

We revised the phase picking manually by using interactive SEISPLUS software. The qualities of the waveforms are relatively high as illustrated in Figure 6. In average, the signal to noise (S/N) ratio from all of the events is 3.2 so the onset of the P and S arrivals are very clear. The picking (timing) uncertainties are defined by weighting parameter values 0, 1, 2, 3 and 4 which correspond to the estimated picking uncertainty of 0 second, 0.05 seconds, 0.1 seconds, 0.15 seconds and 0.2 seconds, respectively. Figure 6 shows the picking process along with phase parameters such as P (t_p) and S (t_s) wave arrival times along with the first motion polarity and error assessment. All of the picking process in this study follows the first motion polarity and error assessment based on the study from Kiehl, T. and Kissling, E., (2007) as described in Table 2. In Figure 6, it can be seen that on the vertical and horizontal channels the picking parameters are 1 P D I and 1 S D I which corresponding to weighting parameter value (1), phase type (P and S stands for P and S wave, respectively), polarity type (U and D or + and - stands for Up and Down, respectively).

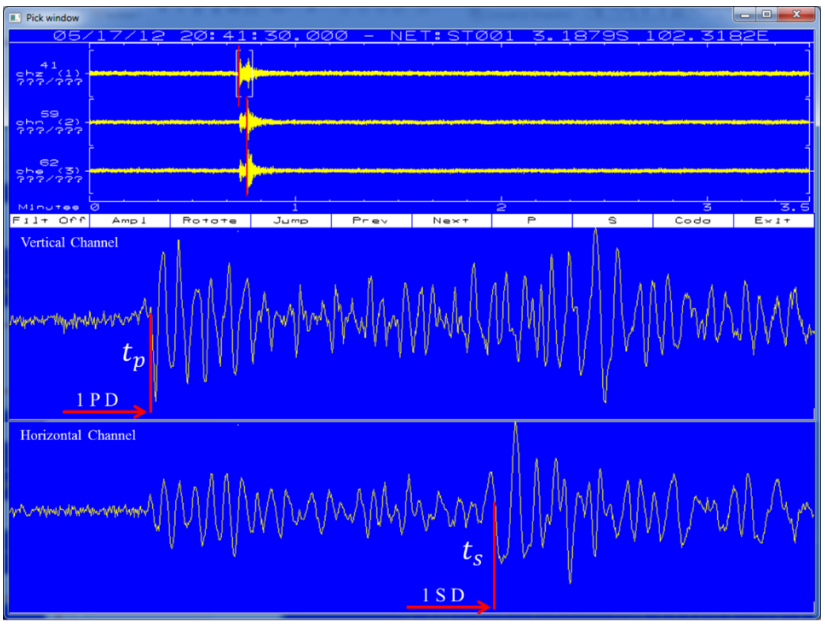

Figure 6 Picking window shows P (t_p) and S (t_s) wave arrival times. The top panel shows the microearthquake event recorded in 3 channels (vertical and horizontal).

Table 2 Summary of error assessment for first motion polarity (from Kiehl, T. and Kissling, E., 2007)

Polarity Label	Polarity is …	Weight
U/D	Up/Down	Polarity is identified with certainty
+/-	Up/Down	Polarity is identified but certaint
N	None	Polarity cannot be identified

6. HYPOCENTER DETERMINATIONS AND RESULTS

For the first step, we determine the hypocenter location by using HYPOPLUS program. The program is utilizes the Geiger iterative method, also known as the Single Event Determination (SED) technique. The result from SED is defined as the initial hypocenter location. Afterwards, we revise and update the hypocenter location by using JHDPLUS program (Oncescu, M.C. and Bonjer, K.P., 1997) by applying the Joint Hypocenter Determination (JHD) technique (Pujol, J., 2000).

Figure 7 shows the comparison of RMS travel time error value from the SED and JHD techniques. On average, the SED and JHD technique has RMS error value equal to 0.15 and 0.11 seconds, respectively. The JHD techniques have smaller RMS error value compared to the SED results which means that the JHD technique is successfully applied in this study. This error value represents the picking quality between the observed and calculated travel time. Based on this calculation, the JHD technique was applied successfully and will be used for further interpretation.

The magnitudes of the MEQ events range from 0.1 up to 2.3. The local earthquake magnitude (M_L) determination is used the Wood-Anderson magnitude calculation (Ellsworth, W. L., 1991). Figure 8 and Figure 9 shows the comparison of epicenter maps and hypocenter distributions based on the results from SED and JHD techniques.

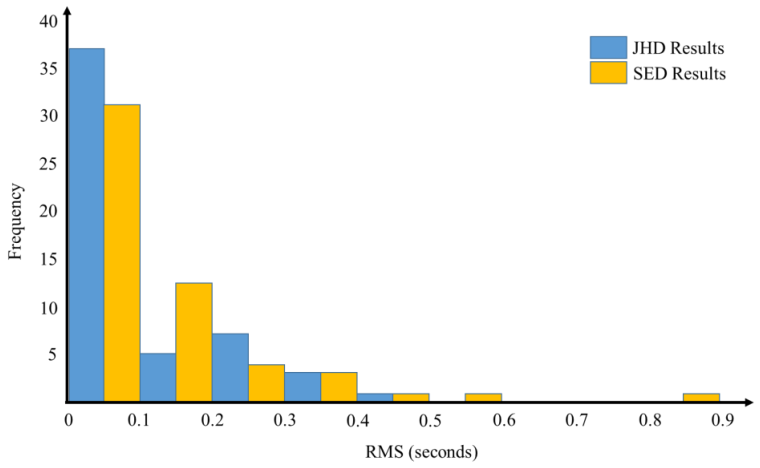

Figure 7 Histogram of RMS travel times value from SED and JHD results.

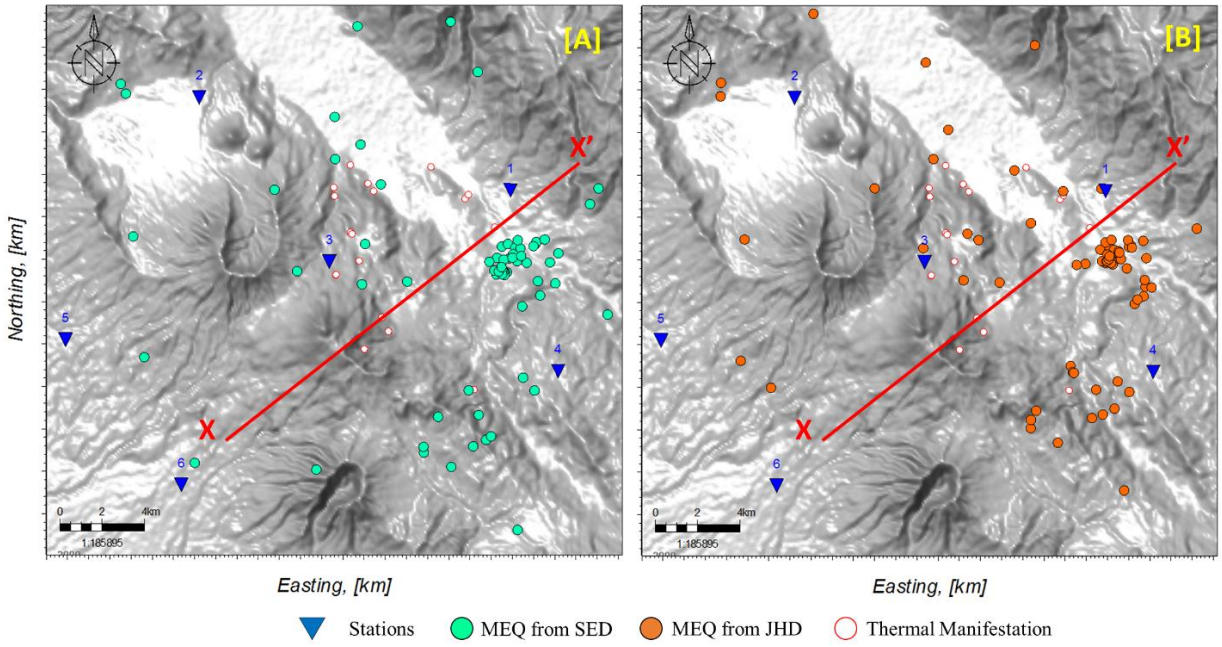

Figure 8 Comparison of epicenter maps showing the results from SED (A) and JHD (B) techniques. The red line (X – X') indicates the vertical section in Figure 9.

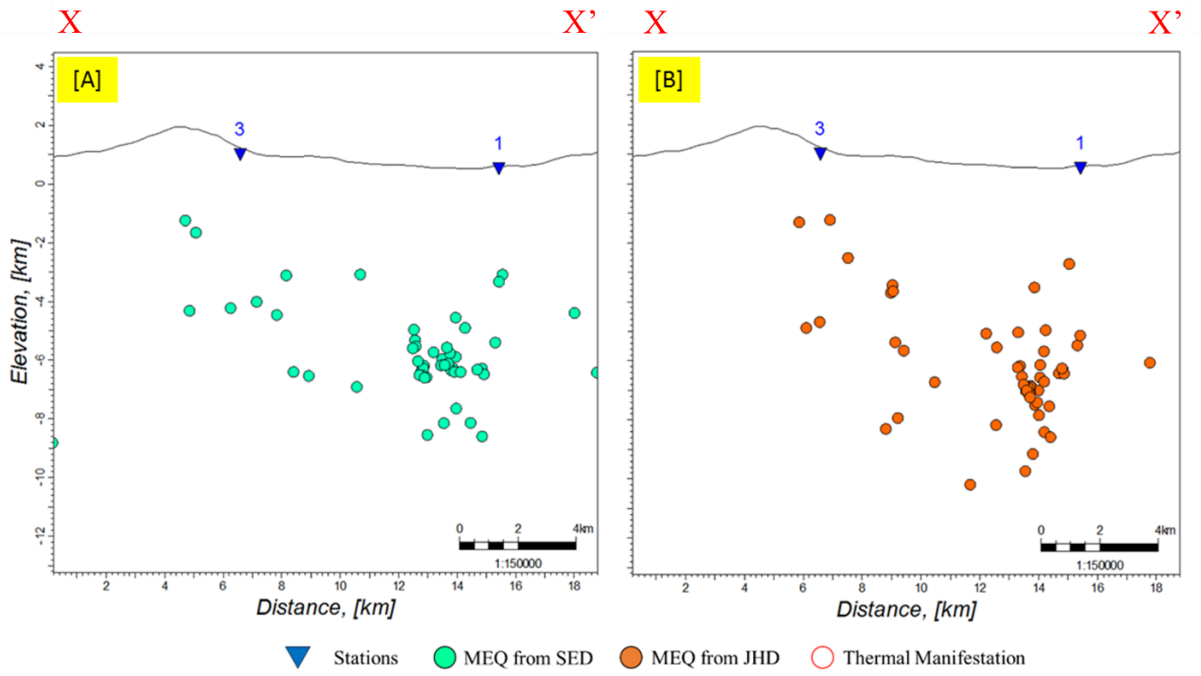

Figure 9 Comparison of hypocenter distributions, showing the results from SED [A] and JHD [B] techniques.

7. ANALYSIS AND INTERPRETATION

7.1 Analysis of SED and JHD Results

In quantitative analysis, the JHD technique successfully revises and updates the hypocenter location by reducing the error parameters. This means that, quantitatively, the JHD result is better than the SED result. If we compare the epicenter maps from SED and JHD result (Figure 8), we could not clearly see which technique has the better result. The MEQ distributions between the two maps are similar. Generally, the events are quite scattered in the central part and rather clustered on the eastern part of the study area. In general practices, the best results from these two techniques are not only defined from statistical result (quantitative) but also from geological perspective (qualitative). In qualitative analysis, the hypocenter distribution (Figure 9) from JHD result gives far more realistic result than the SED. On the JHD result, we could identify some MEQ clusters depicting the fault planes from Sumatran fault system whereas on the SED results we could only identify MEQ cloud without clusters depicting any fault planes.

7.2 Structural Geology Identification Based on MEQ Results

Based on regional geology study, Hululais field is situated within Musi and Ketaun segments of the Sumatran fault system (Sieh K. and Natawidjaja, D., 2000). The Sumatran fault system and its segments have a number of faults planes trending NW – SE. The topographic depression on the North Eastern side of the study area is defined as the Hululais pull-apart basin (Figure 2). This pull-apart basin structure is a product of the right step-over phenomena between the Musi and Ketaun segment. Therefore the Sumatran fault systems within Musi and Ketaun segment are expected as seismically active fault regions. The fault lineaments in Figure 10 [A] were interpreted from satellite images.

Based on the epicenter map, the hypocenter distribution pattern depicts the Sumatran fault system with its associated faults within Musi and Ketaun segments that dominantly have a NW – SE trend. There are also some variations of MEQ events depicting faults lineaments trending NE – SW on the Musi segment (Figure 10 [A]). There is one cluster that has the highest number of MEQ events (about 20 events) on the Ketaun segment. All of the events occurred in a period of 12 hours. These phenomena explain the seismic activity in the Sumatran faults system, especially in the Ketaun segment. The X – X' line corresponds to the vertical section in Figure 10 [B].

Based on the hypocenter distribution (Figure 10 [B]), three clusters of hypocenters are observed with depth varying from 1 to 10 km. One of the MEQ cluster depicts a faulted or fractured zone from the Musi segment. The hypocenter distribution in this cluster is rather scattered so we could not easily interpret the exact position of fault plane, and therefore the interpretation is that it is a fractured zone within the Musi segment. Although with this limitation, the fault orientation and dip is relatively consistent with the regional geological setting that plays part in Musi segment. On the other hand, the other two MEQ clusters reveal two fault planes in the Ketaun segment relatively clearly (see Figure 10 [B]). It appears that the two fault planes have opposite orientations, but similar dip magnitudes. This interpretation is only based on qualitative analysis from the vertical section in Figure 10 [B]. However, in this study we did not perform the seismic source analysis to understand the fault mechanism and to ensure the fault orientation and dip magnitude values. These fault regions with orientation NW – SE within the Musi and Ketaun segments have been regarded as the main exploration drilling target in Hululais geothermal field.

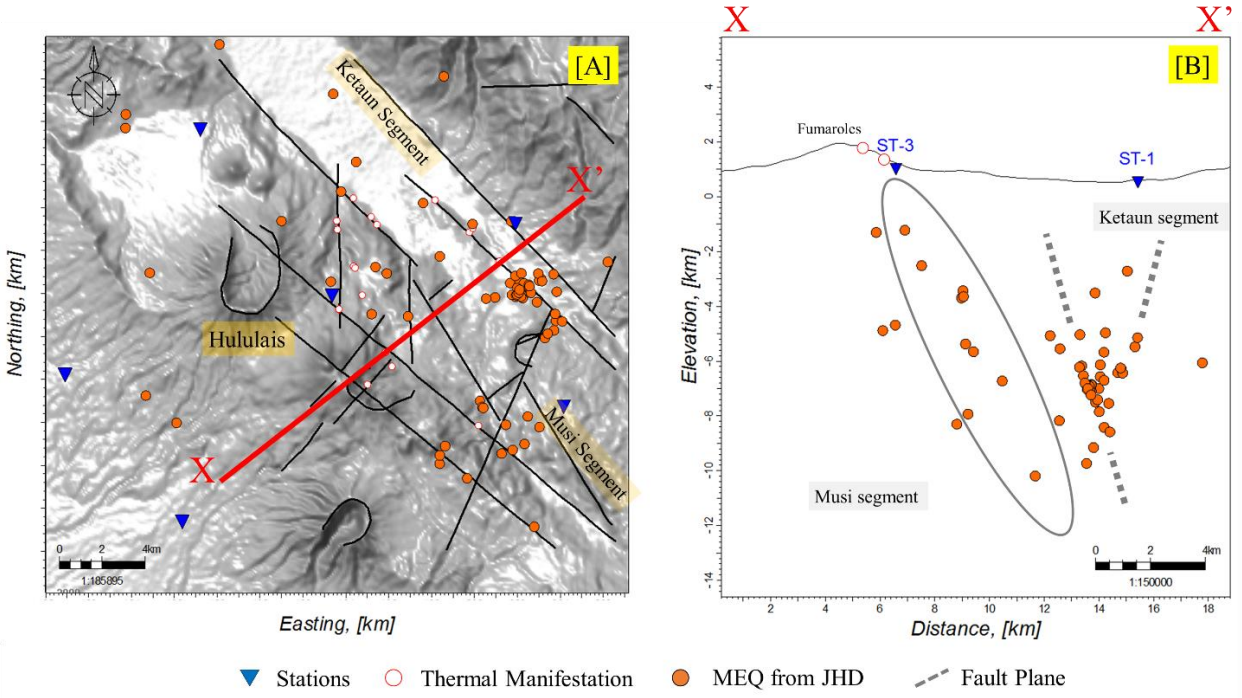

Figure 10 Structural geology interpretation from MEQ distributions, showing the epicenter map [A] and the MEQ hypocenter distribution on vertical section [B].

8. CONCLUSION

The microearthquake (MEQ) monitoring in Hululais field was successfully applied to identify fault and fracture patterns within the Musi and Ketaun segments. A total of about 53 MEQ events were detected. The single event determination (SED) technique is applied to get the initial hypocenter location with average RMS error equal to 0.15 seconds. Then, to improve the accuracy of the hypocenter location, the joint hypocenter determination (JHD) technique is successfully applied, which effectively reduced the average RMS error to 0.11 seconds. Furthermore, the hypocenter distribution from JHD result gives far more realistic qualitative result than the SED. From the JHD result, we could identify several MEQ clusters depicting the fault planes from Sumatran fault system whereas from the SED results we could only identify MEQ clouds without clusters depicting any fault planes. There are three clusters observed with varying depth 1 – 10 km. The clusters from the Musi and Ketaun segment have similar fault orientation (azimuth) while the cluster from Ketaun segment has opposite orientation, but relatively similar dip magnitude.

REFERENCES

Ellsworth, W.L., 1991. The Richter scale ML, from the San Andreas Fault System, California (Professional Paper 1515). USGS. pp. c6, p177.

Kiehl, T. and Kissling, E., 2007. Users Guide for Consistent Phase Picking at Local to Regional Scales. Institute of Geophysics, ETH Zurich, Switzerland.

Muraoka et al., 2010, Geothermal Systems Constrained by the Sumatran Fault and Its Pull-Apart Basins in Sumatra, Western Indonesia, *Proceedings*, 2010 World Geothermal Congress, Bali, Indonesia.

Oncescu, M.C. and Bonjer, K.P., 1997. A note on the depth recurrence and strain release of large Vrancea earthquakes, Tectonophysics, 272, p. 291-302.

Oncescu, M.C., Rizescu, M. and Bonjer, K.P., 1996. SAPS - A completely automated and networked seismological acquisition and processing system. Computer & Geosciences, 22, p. 89-97.

Oncescu, M.C., Rizescu, M., 1997. SAPS v3.0 - Seismological Acquisition and Processing System, User's Guide, Karlsruhe, 82p.

Pujol, J., 2000, Joint Event Location- The JHD Technique and Application to Data From Local Seismic Networks, Advances In Seismic Location, 163–204.